DMD Fast Forward. Published on May 24, 2013 as doi:10.1124/dmd.113.051870

TITLE PAGE

Evidence of drug-drug interactions through uptake and efflux transport systems in rat hepatocytes: implications for cellular concentrations of competing drugs

Youssef Daali, Philippe Millet , Pierre Dayer, and Catherine M Pastor

Service de Pharmacologie et Toxicologie Clinique (DY and DP), Unité de Neurophysiologie Clinique et Neuroimagerie (MP), Laboratoire de Physiopathologie Hépatique et Imagerie Moléculaire, Hôpitaux Universitaires de Genève, Geneva, Switzerland and INSERM U 773, Département de Radiologie, Hôpital Universitaire de Beaujon, Clichy, France (CMP)

RUNNING TITLE PAGE

Drug-drug interactions within hepatocytes

Address for correspondence:

Catherine M. Pastor, M.D., Ph.D.
Laboratoire de Physiopathologie Hépatique et Imagerie Moléculaire
Hôpitaux Universitaires de Genève
Rue Gabrielle-Perret-Gentil, 4
1205 Geneva, Switzerland
Phone: ++41 22 382 38 36
catherine.pastor@hcuge.ch

Number of text pages: 18
Number of tables: 1
Number of figures: 5
Number of references: 54
Number of words in the Abstract: 168
Number of words in the Introduction: 493
Number of words in the Discussion: 1482

LIST OF ABBREVIATIONS

BOPTA	Gadobenate dimeglumine, MultiHance®, Bracco, Milan
DTPA	Gadopentetate dimeglumine, Magnevist®, Bayer Pharma
OATPs	Human Organic Anion Transporting Polypeptides
Oatps	Rat Organic anion transporting polypeptides
MRP2	Human Multiple Resistance-associated Protein 2
Mrp2	Rat Multiple resistance-associated protein 2
RIF	Rifampicin

DMD Fast Forward. Published on May 24, 2013 as DOI: 10.1124/dmd.113.051870
This article has not been copyedited and formatted. The final version may differ from this version.

ABSTRACT

For drugs with hepatobiliary transport across hepatocytes, the interplay between uptake and efflux transporters determines hepatic concentrations of drugs but the evolution over time of these concentrations is difficult to measure in humans, apart from liver imaging with magnetic resonance (MR) contrast agents. Gadobenate dimeglumine (BOPTA, MultiHance®, Bracco, Milan) is a contrast agent used in liver MR imaging that enters into human hepatocytes through Organic Anion Transporting Polypeptides (OATP) and exit unchanged into bile through the Multiple Resistance-associated Protein 2 (MRP2). Rifampicin is transported by the same membrane proteins and may compete with BOPTA for hepatic uptake. Simultaneous drug-drug interactions through uptake and efflux transport systems in hepatocytes according to the cellular concentrations of competing drugs were never investigated. In perfused rat liver preparations, we demonstrate how the drug-drug interactions through transporters determine cellular concentrations of the competing drugs BOPTA and RIF and we show that the cellular concentrations by modulating transport through membranes regulate the rat Oatp-Mrp2 interplay. Moreover, drug interactions through transporters greatly change over time.

INTRODUCTION

In the liver, transporting membrane proteins are major determinants of drug disposition and knowledge on the transport of commercialized compounds and drug candidates is crucial for drug safety and efficacy (Köck and Brouwer, 2012; Yoshida et al., 2013). Transport of drugs across hepatocytes is affected by the changes in expression and function of both sinusoidal and canalicular transporters induced by human diseases, genetic polymorphisms, as well as drug-drug interactions (International Transporter Consortium et al., 2010).

For example, common variants of the *SLCO1B1* gene encoding the Organic Anion Transporting Polypeptide B1 (OATP1B1) are strongly associated with an increased risk of statin-induced myopathy, the loss of uptake function through hepatic OATP1B1 impairing the clearance of statins and favoring the drug accumulation in muscles (SEARCH Collaborative Group et al., 2008). OATP1B1 and OATP1B3 are then uptake transporters of considerable importance for drug disposition (Kalliokoski and Niemi, 2009; Ogasawara et al., 2010; Niemi et al., 2011; Shitara, 2011; Nakanishi and Tamai, 2012). Recently, Karlgren et al. (Karlgren et al., 2012) extensively classified numerous drug competitions through these uptake sinusoidal proteins. Most drugs inhibit the transport of a well-defined substrate specific for each protein but few drugs promote their transport. Once inside hepatocytes, drugs (and metabolites) are excreted into bile through canalicular transporters. Drug-drug interactions and genetic polymorphisms also exist for canalicular proteins such as multiple resistance-associated protein 2 (MRP2) (Keppler, 2011; Oh et al., 2013; Simon et al., 2013).

For drugs with hepatobiliary transport across hepatocytes, the interplay between uptake and efflux transporters determines hepatic concentrations but the evolution over time of these concentrations is difficult to measure in humans, apart from liver imaging with magnetic resonance (MR) contrast agents and tracers (Van Beers et al., 2012). Gadobenate dimeglumine (BOPTA, MultiHance®, Bracco, Milan) and gadoxetate dimeglumine (Gd-EOB-DTPA, Primovist®, Bayer, Berlin) are two contrast agents used in liver MRI that enter into hepatocytes through OATP1B1 and OATP1B3 and exit unchanged into bile through MRP2. Concerns are emerging that liver imaging might be modified by the presence in the sinusoidal blood of organic anions that compete with hepatobiliary contrast agents for entry into hepatocytes. Rifampicin (RIF) is an organic anion that enters into human hepatocytes through OATP1B1 and OATP1B3 and exit into bile through MRP2 and

consequently the drug may compete with other organic anions for hepatic uptake (Lau et al., 2007; Zheng et al., 2009; Karlgren et al., 2012). When chronically administrated, RIF is also a potent inducer of metabolic enzymes and transporters.

Drug-drug interactions through OATP1B1/OATP1B3 and MRP2 proteins are mainly determined by the vascular disappearance of competing drugs over time (Kindla et al., 2009; Kalliokoski and Niemi, 2009; Fahrmayr et al., 2010). Simultaneous drug-drug interactions through uptake and efflux transport systems in hepatocytes were never investigated ex-vivo. The aim of the study was then to elucidate the acute cellular interactions between BOPTA and RIF in perfused rat liver preparations. Only acute transport interactions of RIF were investigated, avoiding the induction of transporters or metabolic enzymes.

DMD Fast Forward. Published on May 24, 2013 as DOI: 10.1124/dmd.113.051870
This article has not been copyedited and formatted. The final version may differ from this version.

MATERIALS AND METHODS

Animals

Normal Sprague-Dawley rats (Charles River, Les Arbreles, France) and rats lacking the canalicular transporter Mrp2 (TR- rats, Division of Clinical Pharmacology and Toxicology, University Hospital of Zurich, Switzerland) were anesthetized with pentobarbital (50 mg · kg^{-1} ip). All animals are male rats. The protocol was approved by the veterinary office in Geneva and followed the guidelines for the care and use of laboratory animals.

Rat liver perfusion

Livers were perfused *in situ* as previously described (Pastor et al., 1996). Briefly, the abdominal cavity was opened and the portal vein was cannulated and secured. The abdominal vena cava was transected and the Krebs-Henseleit-bicarbonate (KHB) solution (118 mM NaCl, 1.2 mM $MgSO_4$, 1.2 mM KH_2PO_4, 4.7 mM KCl, 26 mM $NaHCO_3$, 2.5 mM $CaCl_2$) was pumped without delay into the portal vein. The flow rate was slowly increased over one minute up to 30 ml/min. In a second step, the chest was opened and a second cannula was inserted through the right atrium into the thoracic inferior vena cava and secured. Finally, the ligature around the abdominal inferior vena cava was tightened. The KHB solution was perfused without recirculation to the liver through the portal catheter and eliminated by the catheter placed in the thoracic inferior vena cava. In each experiment, the common bile duct was cannulated with a PE_{10} catheter.

The entire perfusion system included a reservoir, a pump, a device regulating the perfusate temperature to 37°C, a bubble trap, a filter, and an oxygenator. The perfusate was equilibrated with a mixture of 95 % O_2 - 5% CO_2. The livers were perfused with a KHB buffer ± contrast agents and RIF, the concentrations of drugs entering the liver being steady.

Quantification of hepatic concentrations of contrast agents

BOPTA was labeled by adding $^{153}GdCl_3$ (1 MBq/ml) to a 0.5 M BOPTA solution (gadobenate dimeglumine, MultiHance®, Bracco), which contains a slight excess of ligand

(Planchamp et al., 2005a; Planchamp et al., 2005b). The contrast agent was diluted in KHB solution to obtain two concentrations (200 or 1600 µM). To assess the exact intracellular concentrations of BOPTA, Gd-DTPA (Gadopentetate dimeglumine, Magnevist®, Bayer Pharma) was previously perfused at the same concentrations (200 and 1600 µM). DTPA has the same extracellular distribution as BOPTA but does not enter into hepatocytes. To quantify hepatic DTPA and BOPTA, a gamma scintillation probe that measures radioactivity every 20 sec was placed 1 cm above the liver (illustration in Fig. 3). To transform radioactivity counts into contrast agent amounts, the radioactivity in the entire liver at the end of each experiment was measured (Activimeter Isomed 2000, Siemens) and related to the last count measured by the probe. Samples were also collected every 5 min from perfusate and bile to measure the concentrations of labelled drugs.

Experimental protocols

Concentrations of contrast agents in the extracellular space and hepatocytes

To study the hepatic concentrations of the extracellular contrast agent DTPA and BOPTA that also enters into hepatocytes, we perfused livers isolated from normal rats with KHB solution (15 min, recovery period), ^{153}Gd-DTPA (10 min), KHB solution (rinse period, 30 min), ^{153}Gd-BOPTA (30 min), and KHB solution (rinse period, 30 min). During each experiment, we measured hepatic concentrations [nmol/g] and bile flow (µl/min/g) over time. During the drug perfusion and rinse periods, ^{153}Gd-BOPTA bile excretion rate from hepatocytes [nmol/min] was measured every 5 min. During the rinse period (from time 75 to 105 min), no contrast agent enters into hepatocytes and ^{153}Gd-BOPTA measured in outflow perfusate originates from hepatocytes. Thus, during this period, it was possible to assess how the drug is excreted from hepatocytes (efflux back to sinusoids and bile excretion). ^{153}Gd-DTPA perfusion was shorter than ^{153}Gd-BOPTA, because a plateau is rapidly reached. Pharmacokinetic parameters of BOPTA (200 µM) were studied in the absence and in the presence of 100 (n = 3), 10 (n = 3), 1 µM RIF (n = 3), or no RIF (n = 6). Pharmacokinetic

DMD Fast Forward. Published on May 24, 2013 as DOI: 10.1124/dmd.113.051870
This article has not been copyedited and formatted. The final version may differ from this version.

parameters of BOPTA (1600 µM) were also studied in the absence and the presence of 1 µM RIF (n = 3 in each group).

During drug perfusion (from time 45 to time 75 min), ^{153}Gd-BOPTA vascular clearance [nmol/min] was determined every 5 min from the difference of concentrations between inflow (C_{in}) and ouflow (C_{out}) perfusates (C_{in} - C_{out}, nmol/ml) times perfusate flow rate (30 ml/min or 3000 nmol/min). Besides this classical parameter, our model allows a more precise hepatic uptake index because BOPTA concentrations are measured by the gamma probe every 20 seconds over 105 min. We first subtract the hepatic concentrations measured during DTPA perfusion to those obtained during BOPTA to obtain the exact concentrations related to the distribution of BOPTA into hepatocytes. Then, an initial hepatocellular uptake index (IHUI, nmol/min/g) was calculated between time 46 and time 48 min (illustration in Fig. 3). During this 2 min-interval, few BOPTA were excreted into bile and the slope of the relation between concentrations and time accurately reflects the hepatic uptake rate of contrast agent.

Hepatic concentrations of RIF

To study the hepatic concentrations [nmol/g] of RIF (100 µM), we perfused livers isolated from normal rats with KHB solution (45 min, recovery period), RIF (30 min), and KHB solution (rinse period, 30 min). We also measured bile flow (µl/min/g, every 5 min) and RIF bile excretion rates [nmol/min] every 5 min. We measured RIF efflux back to sinusoids [nmol/min] during the rinse period. Hepatic concentrations of RIF was assessed over time, but, in contrast to BOPTA, the extracellular distribution was unknown and the uptake index IHUI was not available because the number of available biopsies were too low. Liver were perfused with RIF 1 µM, 10 µM, or 100 µM RIF and 200 µM BOPTA (n = 10 in each group, including n = 5 for liver biopsies and n = 5 for perfusate and bile sampling). 10 additional rats were used to assess RIF (100 µM) pharmacokinetic parameters in hepatocytes lacking Mrp2.

Liver biopsies were homogenized in 2 ml of methanol. After centrifugation, the supernatants were dried and the residues reconstituted in 200 µl of the mobile phase.

Perfusate samples were directly injected into the high performance liquid chromatography (HPLC) system while bile samples were diluted in water (1:5) before analysis. Separation was carried out on a Zorbax SB-aq C18 column (100 mm × 2.1 mm i.d., particle size 3.5 µm, Agilent) coupled with a guard column with the same stationary phase (20 mm × 2.1 mm i.d, particle size 3.5 µm). The mobile phase consisted of a mixture of ammonium formate 20mM/formic acid 0.1% (A) and acetonitrile (B) (70/30) and was delivered at 0.3 ml/min. Separation was performed under gradient conditions (from 0 to 4 min 70% of B, 4-5 min 70% of B and at 5.5 min return to initial conditions). RIF was quantified using a UV detector (334 nm). Along with the samples, QC and standards samples were processed.

Statistics

Parameters are means ± S.D. Mann Whitney test or Kruskal-Wallis tests were performed to compare the means between different experimental groups.

RESULTS

RIF hepatobiliary transport: effect of BOPTA

During the perfusion of RIF (100 µM over 30 min, from time 45 min to time 75 min), RIF enters into hepatocytes and the vascular clearance (determined from the difference of concentrations between inflow and ouflow perfusates) was maximal at time 50 min (Fig. 1A) and decreased thereafter until time 75 min. Because 3000 nmol/min were perfused (100 µM with a 30-ml/min perfusate flow rate), the extraction ratio was 67% at time 50 min. During this period, RIF bile excretion was < 2 nmol/min (Fig. 1B). The hepatic concentrations steadily increased until the end of RIF perfusion (668 ± 93 nmol/g or µM), RIF uptake being higher than cell excretion (Fig. 1C).

During the rinse period, we can show how RIF is excreted from hepatocytes. Because the extracellular space is completely cleared from RIF within 2 min (see later section), we can assess the efflux rates from hepatocytes back to sinusoids by measuring RIF concentrations in outflow perfusate. During this period, the hepatic concentrations gradually decreased until residual concentrations (197 ± 64 nmol/g or µM, Fig. 1C). The efflux of RIF from hepatocytes back to sinusoids was mainly responsible for this decrease while bile excretion rates remained low (Fig. 1B).

RIF perfusion greatly decreased bile flow with a full recovery when RIF perfusion was stopped and switched to a KHB solution (Fig. 1D). Thus, RIF presence in cells decreased the canalicular transport of intracellular compounds including its own transport, while a recovery of bile flow (Fig. 1D) and RIF bile excretion (Fig. 1B) was observed when RIF hepatic concentrations decreased.

The co-perfusion of 200 µM BOPTA with 100 µM RIF had no effect on vascular clearance (Fig. 1A), bile excretion rates (Fig. 1B), intracellular concentrations of RIF (Fig. 1C), and efflux back to sinusoids (Fig. 1B) because RIF blocked BOPTA uptake and few BOPTA was present in hepatocytes (see next section). Mrp2 mediates the canalicular transport of RIF and hepatocytes lacking Mrp2 are unable to excrete it while hepatic

concentrations were higher in these groups of rats (Table 1). However, perfusate efflux rates were not significantly different in livers with or without Mrp2.

BOPTA hepatobiliary transport: effects of RIF

As observed with RIF, BOPTA uptake clearances were maximal at time 50 min and decreased thereafter (Fig. 2A). With the perfusion of a 200-µM concentration (or 6000 nmol/min), the liver cleared 22% of the contrast agent in a single pass at time 50 min. Besides this classical parameter, an uptake index is available because the gamma probe measures hepatic concentrations each 20 sec (315 measurements over 105 min, Fig. 3A). Moreover, by subtracting the concentrations induced by the perfusion of the extracellular contrast agent DTPA, we can quantify the exact concentrations of BOPTA in hepatocytes (Fig. 3B and D). All radioactivity of DTPA was cleared from the liver by the KHB solution within 2 min (Fig. 3A). An initial hepatocellular uptake index (IHUI, nmol/min/g) was calculated between time 46 and time 48 min (46 ± 6 nmol/min/g, Fig. 3D). During this 2 min-interval, a limited amount of BOPTA was excreted into bile and the slope of the relation between concentrations and time accurately reflects the hepatic uptake rate of the contrast agent. Later the hepatic concentrations do not measure the hepatocellular uptake but rather the combination of drug uptake into hepatocytes and exit out of cells. The concentrations in hepatocytes constantly increase until the end of BOPTA perfusion, drug uptake being higher than drug elimination (Fig 2D). During this period, bile excretion rates (Fig. 2B) and bile flow (not shown) were high. During the following rinse period, BOPTA exited from hepatocytes mainly through the canalicular membrane (Fig. 2B) while the efflux rates to sinusoids were much lower (Fig. 2C).

When RIF was co-perfused with BOPTA (200 µM), the uptake index IHUI significantly decreased with increasing concentrations of perfused RIF (Fig. 3D). RIF (10 and 100 µM) nearly blocked BOPTA entry into hepatocytes (Fig. 2D). With a lower concentration of RIF (1 µM), the cellular concentrations of BOPTA increased, reached a plateau by time 54 min and then slightly decreased until time 75 min (Fig. 2D). Such decrease is explained by excretion

DMD Fast Forward. Published on May 24, 2013 as DOI: 10.1124/dmd.113.051870
This article has not been copyedited and formatted. The final version may differ from this version.

rates being higher than uptake rates. During the rinse period, hepatic concentrations of BOPTA decreased to the residual concentrations (47 ± 7 nmol/g).

Can 1600 µM BOPTA overcome the uptake inhibition induced by 1 µM RIF?

Interactions being potentially concentration-dependent, we perfused livers with 1600 µM BOPTA to overcome the effect of RIF 1 µM on the transport of 200 µM BOPTA. Concentrations within hepatocytes were slightly higher during the perfusion of 1600 µM BOPTA and 1 µM RIF than during the perfusion of 200 µM alone but much lower than during the perfusion of 1600 µM BOPTA alone (Fig. 4B). The uptake index IHUI were not significantly different between 1600 µM BOPTA (151 ± 22 nmol/min/g) and 1600 µM BOPTA and 1 µM RIF (110 ± 33 nmol/min/g, p = 0.20) but higher than during the perfusion of 200 µM BOPTA (46 ± 6 nmol/min/g). BOPTA entry into hepatocytes was similar at the beginning of the perfusion (Fig. 4B) in the two groups and BOPTA concentrations increased until time 54 min when concentrations reached a plateau in the group perfused with 1 µM. Then, in this group, from time 54 to the end of perfusion, uptake rates became similar to excretion rates. Because from time 54 to time 75 min, bile excretion rates decreased (Fig. 4A), the uptake rates should have similar evolution. During the rinse period, BOPTA bile excretion rates decreased with the cellular concentrations while BOPTA efflux back to sinusoids were higher in the presence of RIF (Fig. 4C).

Drug-drug interactions through uptake, bile excretion, and efflux transport systems in hepatocytes

No effect of BOPTA perfused at 200 µM was shown on 100 µM RIF transport because few contrast agents entered into hepatocytes (Fig. 1). The competition of RIF on BOPTA transport was more informative. It was easy to evidence how RIF impeded BOPTA entry into hepatocytes by the uptake index IHUI (Fig. 3D) or the vascular clearances (Fig. 2A). RIF had priority over BOPTA for uptake through rat Oatps. When 1600 µM BOPTA was

perfused with 1 µM RIF, the initial uptake index was unchanged but impaired uptake appeared by time 54 min.

The drug-drug interactions through exit transporters are more difficult to measure because cell excretion depends on concentrations in hepatocytes. We then plotted the excretion rates in relation to BOPTA cellular concentrations in all experimental groups according to RIF presence or absence (Fig. 5). Bile excretion rates increased with the cellular concentrations of BOPTA until a limit of 1000 - 1200 µM. Thereafter bile excretion rates remained constant. The presence of RIF in hepatocytes did not interfere with this relationship (Fig. 5A and 5B). In contrast, the perfusate efflux rates were significantly higher in the presence of RIF and at similar concentrations of BOPTA, the efflux rates back to perfusate were higher in the presence of RIF (Fig. 5C). The high efflux of RIF back to sinusoids at various cellular concentrations (Table 1) probably promotes the transport of BOPTA.

DISCUSSION

For years, information on the hepatobiliary transport of drugs and drug-drug interactions was mainly obtained by measuring vascular clearance or drug disappearance from sinusoidal blood. However, we hypothesized that measuring hepatic concentrations over time would bring more information for various reasons: 1) The hepatic concentrations of MR contrast agents correlate with images and recent liver imaging with hepatobiliary contrast agents was used to assess OATP1B1 and OATP1B3 polymorphisms (Nassif et al., 2012); 2) The importance of drug concentrations acting within hepatocytes such as statins is obvious (Rodrigues, 2010); and 3) the metabolism of drugs depends on hepatic concentrations (metabolizing enzymes-transport interplay) (Benet, 2009; Zhang et al., 2009). Nevertheless, apart from liver imaging with contrast agents and tracers, cellular pharmacokinetics is difficult to assess in humans. The novelty of our study was then to present drug-drug interactions through uptake and efflux transport systems between two drugs with different hepatobiliary behavior. The interactions were studied in perfused rat livers because it is easy to control hepatic perfusate flow (set to 30 ml/min). The composition of perfused solutions is well controlled and interference with extrahepatic organs is avoided by liver isolation. During the perfusion of drugs, only bile excretion rates were assessed because drug concentrations measured in outflow perfusate do not distinguish molecules coming from hepatocytes from those not taken up. In contrast, following a 5-min perfusion of KHB (long enough to rinse the entire extracellular space), all molecules measured in outflow perfusate originate from hepatocytes. We can then compare, how RIF and BOPTA exit from hepatocytes and whether interactions exist through transporters.

The cellular transport of RIF is incompletely known. RIF enters into human hepatocytes through OATP1B1 and OATP1B3 (Vavricka et al., 2002; Tirona et al., 2003; Vavricka et al., 2004). We show that RIF is mainly excreted by efflux back to the systemic circulation. Few RIF is excreted into bile through rat Mrp2. During RIF perfusion, a steady increase of cellular concentrations show that uptake rates are higher than excretion rates.

The extraction ratio is 67% during a single pass 5 min after the start of perfusion but decreases thereafter. RIF accumulation into hepatocytes decreases bile flow below the baseline value, emphasizing the cholestatic effect of the drug at a 100 µM-concentration (Stieger et al., 2000). Recovery of impaired bile flow is rapid when hepatic RIF concentrations decrease. Such finding may explain the early hepatocellular dysfunction associated with RIF treatment in patients (Tostmann et al., 2008). The cellular mechanisms of cholestasis associate interactions with drug uptake in mice (van de Steeg et al., 2010 ; Neyt et al., 2013) as well as decreased bile excretion through Mrp2 in mice (Neyt et al., 2013) and the human Bile Salt Export Pump in transfected cells (Mita et al., 2006). However, RIF has also beneficial effects in cholestatic liver diseases, chronic treatment with RIF enhancing bile acid detoxification and bilirubin conjugation and excretion in association with an increased hepatic expression of CYP3A4, UGT1A1, and MRP2 (Marschall et al., 2005). During the rinse period, we show that RIF mainly exits from hepatocytes through the sinusoidal membrane. However, the mechanism of such efflux into sinusoids is unknown. RIF (as well as BOPTA) may use Oatps that are bidirectional or Mrp transporters of the sinusoidal membrane (Li et al., 2000).

We know that BOPTA distributes to the extracellular space and enters into rat hepatocytes through the sinusoidal transporters Oatp1a1, Oatp1a4, and Oatp1b2 (Planchamp et al., 2007). The V_{max} of maximal BOPTA accumulation was 2133 nmol/g/30 min in normal livers and 2945 nmol/g/30 min in livers lacking Mrp2 (Millet et al., 2011). BOPTA is excreted unchanged into bile through Mrp2 and rats lacking Mrp2 do not excrete BOPTA (de Haën et al., 1999; Millet et al., 2011). The time for BOPTA to reach bile is ≤ 5 min as observed with the bile salt taurocholate (Crawford et al., 1988). BOPTA bile excretion increases bile flow, the transport of BOPTA through hepatocytes driving water across membranes (Tietz et al., 2005; Mottino et al., 2006; Lehmann et al., 2008). Similarly to RIF, BOPTA effluxes back to sinusoids but the contrast agent is mainly excreted from hepatocytes by bile excretion. Interestingly, bile excretion rates rely on hepatic concentrations until a threshold value of 1000 - 1200 nmol/g. Perfusate excretion rates are

also related to cellular concentrations (Millet et al., 2011).

The cellular drug-drug interactions of BOPTA and RIF are dose and time-dependent. BOPTA (200 µM) is not taken up and does not interfere with the hepatobiliary transport of RIF until the concentrations of RIF in sinusoids decrease to 1 µM. Moreover, RIF (1 µM) does not modify the uptake index IHUI of 1600 µM BOPTA until RIF finds the way through transporters and decreases BOPTA uptake (by time 54 min). Then, the concentrations within hepatocytes stop to increase and remain steady, uptake and excretion rates being similarly decreased. In contrast, with a perfusion of 200 µM BOPTA, RIF decreases the IHUI as early as 2 min after the start of perfusions. RIF is likely to inhibit BOPTA entry through the rat Oatp1a4 rather than through Oatp1a1 (Fattinger et al., 2000).

Competition for BOPTA and RIF uptake transport may rely on the physicochemical structures of drugs (such as lipophilicity and polar surface area) as recently published by Karlgren at al. (Karlgren et al., 2012). As shown in the present study, drug concentrations are also important determinants of drug-drug interactions. Over time, the increase of drug concentrations in hepatocytes might modulate uptake through Oatps, the concentration gradient across membrane decreasing with a constant concentrations in inflow perfusate and increasing concentrations inside cells. With perfused rat livers in the MRI room, we also showed that bromosulfophthalein blocks the uptake of BOPTA into hepatocytes (Pastor et al., 2003).

To evidence whether drug-drug interactions occur through efflux transport systems, we plotted the efflux rates against cellular concentrations. With BOPTA, efflux rates and hepatic concentrations are available every 5 min. For RIF only two intracellular concentrations (90 and 105 min) are available. Interestingly, RIF did not interfere with the transport of BOPTA through Mrp2 and the low bile excretion rates of RIF may explain the absence of interaction with BOPTA through Mrp2. In contrast, RIF increases the sinusoidal efflux rates of BOPTA for a given concentration, a finding in line with the high efflux back of RIF to sinusoids. Karlgren at al. (Karlgren et al., 2012) also show that a few compounds may stimulate transport of a test drug through OATP1B1 and OATP1B3. Similar results were

observed through MRP2 where interacting compounds may serve as both stimulators and inhibitors depending on concentrations used (Zelcer et al., 2003).

Extrapolating our data to the clinical situation, it is likely that if patients treated with RIF need a liver MRI, RIF uptake into hepatocytes would be favored until blood RIF concentrations decrease to 1 µM. In patients, the therapeutic concentrations of RIF in serum are in the range of 5 to 10 µM with unbound concentrations of 1-2 µM for sinusoidal uptake (Acocella, 1983). No toxicity with RIF is then anticipated because RIF has priority over BOPTA. Extrahepatic toxicity of BOPTA is unlikely, but delayed hepatobiliary clearance of the contrast agent will compromise liver imaging. When Kato el al. (Kato et al., 2002) inject Gd-EOB-DTPA (6.25 µmol, iv) 30 min after RIF (40 mg/kg or 12 µmol, iv), the contrast agent did not enter into hepatocytes and the exam was useless. Other acute drug-drug interactions have been published. The concomitant iv administration of RIF (600 mg/kg) increases the plasma concentrations of atorvastatin (Lau et al., 2007). Atorvasatatin was cleared from blood within 24 hours but delayed hepatobiliary clearance may induce myopathy.

Drug-drug interactions in pharmacological studies are mainly determined by the kinetics of drug plasma disappearance. Such clearance methods are useful in clinical practice but do not convey all the information, including hepatic concentrations. Consequently, physiologically based pharmacokinetic models and mathematical simulations were used to show how alterations in the transport through hepatic transporters can modify the concentrations of drugs (Shitara and Sugiyama, 2006; Kusuhara and Sugiyama, 2009; Watanabe et al., 2009; Watanabe et al., 2010). However, in these studies, pharmacokinetic modeling and simulations estimate hepatocellular concentrations in contrast to our model in which, all parameters are measured. Besides liver MRI, positron emission tomography (PET) imaging with [^{14}C]telmisartan of the liver can also evidence the accumulation of the tracer in rat livers while PET imaging with (15R)-11C-TIC-Me assesses the hepatobiliary transport in humans (Takashima et al., 2011; Takashima et al., 2012). We recently showed the pharmacokinetics of BOPTA in cholestatic fatty rat livers with compartmental analysis and

simulations in relation to the transport function across membrane transporters (Pastor et al., 2013).

In conclusion, our study demonstrates how the drug-drug interactions through transporters determine cellular concentrations of competing drugs and shows that cellular concentrations by modulating transport through membranes regulate the rat Oatp-Mrp2 interplay. Moreover, drug interactions through transporters greatly change over time.

ACKNOWLEDGMENTS

The authors thank Bruno Stieger (Clinical Pharmacology and Toxicology, University Hospital, Zürich, Switzerland) for providing rats lacking Mrp2.

AUTHORSHIP CONTRIBUTIONS

Participated in research design: Daali, Millet, Dayer, Pastor

Conducted experiments: Daali, Millet, Dayer, Pastor

Contributed new reagents or analytic tools: Daali

Performed data analysis: Daali, Millet, Dayer, Pastor

Wrote or contributed to the writing of the manuscript: Daali, Millet, Dayer, Pastor

REFERENCES

Acocella G (1983) Pharmacokinetics and metabolism of rifampin in humans. *Rev. Infect. Dis.* **5:**S428-S432.

Benet LZ (2009) The drug transporter-metabolism alliance: uncovering and defining the interplay. *Mol. Pharm.* **6:**1631-1643.

Crawford JM, Berken CA and Gollan JL (1988) Role of the hepatocyte microtubular system in the excretion of bile salts and biliary lipid: implications for intracellular vesicular transport. *J. Lipid Res.* **29:**144-156.

de Haën C, La Ferla R and Maggioni F (1999) Gadobenate dimeglumine 0.5 M solution for injection (MultiHance) as contrast agent for magnetic resonance imaging of the liver : mechanistic studies in animals. *J. Comput. Assist. Tomogr.* **23:**S169-S179.

Fahrmayr C, Fromm MF and König J (2010) Hepatic OATP and OCT uptake transporters: their role for drug-drug interactions and pharmacogenetic aspects. *Drug Metab. Rev.* **42:**380-401.

Fattinger K, Cattori V, Hagenbuch B, Meier PJ and Stieger B (2000) Rifamycin SV and rifampicin exhibit differential inhibition of the hepatic rat organic anion transporting polypeptides, Oatp1 and Oatp2. *Hepatology* **32:**82-86.

International Transporter Consortium, Giacomini KM, Huang SM, Tweedie DJ, Benet LZ, Brouwer KL, Chu X, Dahlin A, Evers R, Fischer V, Hillgren KM, Hoffmaster KA, Ishikawa T, Keppler D, Kim RB, Lee CA, Niemi M, Polli JW, Sugiyama Y, Swaan PW, Ware JA, Wright SH, Yee SW, Zamek-Gliszczynski MJ and Zhang L (2010) Membrane transporters in drug development. *Nat. Rev. Drug Discov.* **9:**215-236.

Kalliokoski A and Niemi M (2009) Impact of OATP transporters on pharmacokinetics. *Br. J. Pharmacol.* **158:**693-705.

Karlgren M, Vildhede A, Norinder U, Wisniewski JR, Kimoto E, Lai Y, Haglund U and Artursson P (2012) Classification of inhibitors of hepatic organic anion transporting polypeptides (OATPs): influence of protein expression on drug-drug interactions. *J. Med. Chem.* **55:**4740-4763.

Kato N, Yokawa T, Tamura A, Heshiki A, Ebert W and Weinmann HJ (2002) Gadolinium-ethoxybenzyl-diethylenetriamine-pentaacetic acid interaction with clinical drugs in rats. *Invest. Radiol.* **37:**680-684.

Keppler D (2011) Multidrug resistance proteins (MRPs, ABCCs): importance for pathophysiology and drug therapy. *Handb. Exp. Pharmacol.* **201:**299-323.

Kindla J, Fromm MF and König J (2009) In vitro evidence for the role of OATP and OCT uptake transporters in drug-drug interactions. *Expert Opin. Drug Metab. Toxicol.* **5:**489-500.

Köck K and Brouwer KL (2012) A perspective on efflux transport proteins in the liver. *Clin. Pharmacol. Ther.* **92:**599-612.

Kusuhara H and Sugiyama Y (2009) In vitro-in vivo extrapolation of transporter-mediated clearance in the liver and kidney. *Drug Metab. Pharmacokinet.* **24:**37-52.

Lau YY, Huang Y, Frassetto L and Benet LZ (2007) Effect of OATP1B transporter inhibition on the pharmacokinetics of atorvastatin in healthy volunteers. *Clin. Pharmacol. Ther.* **81:**194-204.

Lehmann GL, Larocca MC, Soria LR and Marinelli RA (2008) Aquaporins: their role in cholestatic liver disease. *World J. Gastroenterol.* **14:**7059-7067.

Li L, Meier PJ and Ballatori N (2000) Oatp2 mediates bidirectional organic solute transport: a role for intracellular glutathione. *Mol. Pharmacol.* **58:**335-340.

Marschall HU, Wagner M, Zollner G, Fickert P, Diczfalusy U, Gumhold J, Silbert D, Fuchsbichler A, Benthin L, Grundström R, Gustafsson U, Sahlin S, Einarsson C and Trauner M (2005) Complementary stimulation of hepatobiliary transport and detoxification systems by rifampicin and ursodeoxycholic acid in humans. *Gastroenterology* **129:**476-485.

Millet P, Moulin M, Stieger B, Daali Y and Pastor CM (2011) How organic anions accumulate in hepatocytes lacking Mrp2: evidence in rat liver. *J. Pharmacol. Exp. Ther.* **336:**624-632.

Mita S, Suzuki H, Akita H, Hayashi H, Onuki R, Hofmann AF and Sugiyama Y (2006) Inhibition of bile acid transport across Na+/taurocholate cotransporting polypeptide (SLC10A1) and bile salt export pump (ABCB 11)-coexpressing LLC-PK1 cells by cholestasis-inducing drugs. *Drug Metab. Dispos.* **34:**1575-1581.

Mottino AD, Carreras FI, Gradilone SA, Marinelli RA and Vore M (2006) Canalicular membrane localization of hepatocyte aquaporin-8 is preserved in estradiol-17beta-D-glucuronide-induced cholestasis. *J Hepatol.* **44:**232-233.

Nakanishi T and Tamai I (2012) Genetic polymorphisms of OATP transporters and their impact on intestinal absorption and hepatic disposition of drugs. *Drug Metab. Pharmacokinet.* **27:**106-121.

Nassif A, Jia J, Keiser M, Oswald S, Modess C, Nagel S, Weitschies W, Hosten N, Siegmund W and Kühn JP (2012) Visualization of hepatic uptake transporter function in healthy subjects by using gadoxetic acid-enhanced MR imaging. *Radiology* **264:**741-750.

Neyt S, Huisman MT, Vanhove C, De Man H, Vliegen M, Moerman L, Dumolyn C, Mannens G and De Vos F (2013) In vivo visualization and quantification of (disturbed) Oatp-mediated hepatic uptake and Mrp2-mediated biliary excretion of 99mTc-mebrofenin in mice. *J. Nucl. Med.* **54:**624-630.

Niemi M, Pasanen MK and Neuvonen PJ (2011) Organic anion transporting polypeptide 1B1: a genetically polymorphic transporter of major importance for hepatic drug uptake. *Pharmacol. Rev.* **63:**157-181.

Ogasawara K, Terada T, Katsura T, Hatano E, Ikai I, Yamaoka Y and Inui K (2010) Hepatitis C virus-related cirrhosis is a major determinant of the expression levels of hepatic drug transporters. *Drug Metab. Pharmacokinet.* **25:**190-199.

Oh ES, Kim CO, Cho SK, Park MS and Chung JY (2013) Impact of ABCC2, ABCG2 and SLCO1B1 polymorphisms on the pharmacokinetics of pitavastatin in humans. *Drug Metab. Pharmacokinet. in press*

Pastor CM, Planchamp C, Pochon S, Lorusso V, Montet X, Mayer J, Terrier F and Vallée J-P (2003) Kinetics of gadobenate dimeglumine in isolated perfused rat liver: MR imaging evaluation. *Radiology* **229:**119-125.

Pastor CM, Wiliams D, Yoneyama T, Hatakeyama K, Singleton S, Naylor E and Billiar TR (1996) Competition for tetrahydrobiopterin between phenylalanine hydroxylase and nitric oxide synthase in rat liver. *J. Biol. Chem.* **271:**24534-24538.

Pastor CM, Wissmeyer M and Millet P (2013) Concentrations of Gd-BOPTA in cholestatic fatty rat livers: role of transport functions through membrane proteins. *Contrast Media Molecular Imaging* **8:**147-156.

Planchamp C, Beyer GJ, Slosman DO, F Terrier F and Pastor CM (2005a) Direct evidence of the temperature dependence of Gd-BOPTA transport in the intact liver. *Applied Radiations and Isotopes* **62:**943-949.

Planchamp C, Hadengue A, Stieger B, Bourquin J, Vonlaufen A, Frossard J-L, Quadri R, Becker CD and Pastor CM (2007) Function of both sinusoidal and canalicular transporters controls the concentration of organic anions within hepatocytes. *Mol. Pharmacol.* **71:**1089-1097.

Planchamp C, Pastor CM, Balant L, Becker CD, Terrier F and Gex-Fabry M (2005b) Quantification of Gd-BOPTA uptake and biliary excretion from dynamic MRI in rat livers: model validation with ^{153}Gd-BOPTA. *Invest. Radiol.* **40:**705-714.

Rodrigues AC (2010) Efflux and uptake transporters as determinants of statin response. *Expert Opin. Drug Metab. Toxicol.* **6** 621-632.

SEARCH Collaborative Group, Link E, Parish S, Armitage J, Bowman L, Heath S, Matsuda F, Gut I, Lathrop M and Collins R (2008) SLCO1B1 variants and statin-induced myopathy--a genomewide study. *N. Engl. J Med.* **359:**789-799.

Shitara Y (2011) Clinical importance of OATP1B1 and OATP1B3 in drug-drug interactions. *Drug Metab. Pharmacokinet.* **26:**220-227.

Shitara Y and Sugiyama Y (2006) Pharmacokinetic and pharmacodynamic alterations of 3-hydroxy-3-methylglutaryl coenzyme A (HMG-CoA) reductase inhibitors: drug-drug

interactions and interindividual differences in transporter and metabolic enzyme functions. *Pharmacol. Ther.* **112:**71-105.

Simon N, Marsot A, Villard E, Choquet S, Khe HX, Zahr N, Lechat P, Leblond V and Hulot JS (2013) Impact of ABCC2 polymorphisms on high-dose methotrexate pharmacokinetics in patients with lymphoid malignancy. *Pharmacogenomics J.*

Stieger B, Fattinger K, Madon J, Kullak-Ublick GA and Meier PJ (2000) Drug- and estrogen-induced cholestasis through inhibition of the hepatocellular bile salt export pump (Bsep) of rat liver. *Gastroenterology* **118:**422-430.

Takashima T, Hashizume Y, Katayama Y, Murai M, Wada Y, Maeda K, Sugiyama Y and Watanabe Y (2011) The Involvement of organic anion transporting polypeptide in the hepatic uptake of telmisartan in rats: PET studies with [(11)C]telmisartan. *Mol. Pharm.* **8:**1789-1798.

Takashima T, Kitamura S, Wada Y, Tanaka M, Shigihara Y, Ishii H, Ijuin R, Shiomi S, Nakae T, Watanabe Y, Cui Y, Doi H, Suzuki M, Maeda K, Kusuhara H, Sugiyama Y and Watanabe Y (2012) PET imaging-based evaluation of hepatobiliary transport in humans with (15R)-11C-TIC-Me. *J. Nucl. Med.* **53:**741-748.

Tietz P, Jefferson J, Pagano R and LaRusso NF (2005) Membrane microdomains in hepatocytes: potential target areas for proteins involved in canalicular bile secretion. *J. Lipid Res.* **46:**1426–1432.

Tirona RG, Leake BF, Wolkoff AW and Kim RB (2003) Human organic anion transporting polypeptide-C (SLC21A6) is a major determinant of rifampin-mediated pregnane X receptor activation. *J. Pharmacol. Exp. Ther.* **304:**223-228.

Tostmann A, Boeree MJ, Aarnoutse RE, de Lange WC, van der Ven AJ and Dekhuijzen R (2008) Antituberculosis drug-induced hepatotoxicity: concise up-to-date review. *J. Gastroenterol. Hepatol.* **23:**192-202.

Van Beers BE, Pastor CM and Hussain HK (2012) Primovist, Eovist: what to expect? *J. Hepatol.* **57:**421-429.

van de Steeg E, Wagenaar E, van der Kruijssen CM, Burggraaff JE, de Waart DR, Elferink RP, Kenworthy KE and Schinkel AH (2010) Organic anion transporting polypeptide 1a/1b-knockout mice provide insights into hepatic handling of bilirubin, bile acids, and drugs. *J. Clin. Invest.* **120:**2942-2952.

Vavricka SR, Jung D, Fried M, Grützner U, Meier PJ and Kullak-Ublick GA (2004) The human organic anion transporting polypeptide 8 (SLCO1B3) gene is transcriptionally repressed by hepatocyte nuclear factor 3beta in hepatocellular carcinoma. *J. Hepatol.* **40:**212-218.

Vavricka SR, Van Montfoort J, Ha HR, Meier PJ and Fattinger K (2002) Interactions of rifamycin SV and rifampicin with organic anion uptake systems of human liver. *Hepatology* **36:**164-172.

Watanabe T, Kusuhara H, Maeda K, Shitara Y and Sugiyama Y (2009) Physiologically based pharmacokinetic modeling to predict transporter-mediated clearance and distribution of pravastatin in humans. *J. Pharmacol. Exp. Ther.* **328:**652-662.

Watanabe T, Kusuhara H and Sugiyama Y (2010) Application of physiologically based pharmacokinetic modeling and clearance concept to drugs showing transporter-mediated distribution and clearance in humans. *J. Pharmacokinet. Pharmacodyn.* **37:**575-590.

Yoshida K, Maeda K and Sugiyama Y (2013) Hepatic and intestinal drug transporters: prediction of pharmacokinetic effects caused by drug-drug interactions and genetic polymorphisms. *Annu. Rev. Pharmacol. Toxicol.* **53:**581-612.

Zelcer N, Huisman MT, Reid G, Wielinga P, Breedveld P, Kuil A, Knipscheer P, Schellens JH, Schinkel AH and Borst P (2003) Evidence for two interacting ligand binding sites in human multidrug resistance protein 2 (ATP binding cassette C2). *J. Biol. Chem.* **278:**23538-23544.

Zhang L, Zhang Y and Huang SM (2009) Scientific and regulatory perspectives on metabolizing enzyme-transporter interplay and its role in drug interactions: challenges in predicting drug interactions. *Mol. Pharm.* **6:**1766-1774.

Zheng HX, Huang Y, Frassetto LA and Benet LZ (2009) Elucidating rifampin's inducing and inhibiting effects on glyburide pharmacokinetics and blood glucose in healthy volunteers: unmasking the differential effects of enzyme induction and transporter inhibition for a drug and its primary metabolite. *Clin. Pharmacol. Ther.* **85:**78-85.

FOOTNOTES

The Fonds National Suisse de la Recherche Scientifique [N° 310030-126030] and the Boninchi Foundation of Geneva, Switzerland [N° ME9117] supported the work.

LEGENDS FOR FIGURES

Fig. 1. Rifampicin (RIF) transport through hepatocytes. A. Vascular clearances [nmol/min] are quantified from the difference of concentrations between inflow and outflow perfusates [nmol/ml] times perfusate flow rates (30 ml/min). RIF concentrations in inflow perfusate were 100 µM or 3000 nmol/min. Livers isolated from normal rats were perfused with a Krebs-Henseleit Bicarbonate (KHB) solution (from 0 to 45 min), 100 µM RIF ± BOPTA (from 45 to 75 min), and KHB solution (from 75 to 105 min): 100 µM RIF (white squares) or 100 µM RIF and 200 µM BOPTA (grey squares). B. Efflux rates of RIF from hepatocytes back to sinusoids and bile excretion rates [nmol/min] were measured. Concentrations in hepatocytes ~~(HC)~~ [nmol/g, C] and bile flow [µl/min/g, D] in both groups over time. Vertical lines limit the period of drug perfusion.

Fig. 2. BOPTA transport through hepatocytes. A. Vascular clearances [nmol/min] are quantified from the difference of concentrations between inflow and outflow perfusates [nmol/ml] times perfusate flow rates (30 ml/min). BOPTA concentrations in inflow perfusate were 200 µM or 6000 nmol/min. Livers isolated from normal rats were perfused with a Krebs-Henseleit Bicarbonate (KHB) solution (from 0 to 45 min), 200 µM BOPTA ± rifampicin (RIF) (from 45 to 75 min), and KHB solution (from 75 to 105 min): 200 µM BOPTA alone (white squares) and 100 µM RIF (heavy grey), 10 µM RIF (light grey), or 1 µM RIF (black squares). BOPTA bile excretion rates [nmol/min, B], BOPTA efflux rates from hepatocytes back to sinusoids [nmol/min, C], and BOPTA concentrations in hepatocytes [nmol/g] (D) are illustrated. In Fig 2D, BOPTA concentrations in extracellular space was substracted from liver concentrations to quantify BOPTA in hepatocytes (see next figure). Vertical lines limit the period of drug perfusion.

Fig. 3. A. On line recording of contrast agents by the gamma scintillation probe placed 1 cm over the liver, which measures the hepatic count rates. Livers were perfused with DTPA

(time 0 to time 10 min), KHB solution (time 10 to time 45 min), BOPTA (time 45 to time 75 min), and KHB solution (time 75 to time 105 min). B and C. To assess the hepatic concentrations in hepatocytes [nmol/g], concentrations induced by the extracellular distribution of DTPA were subtracted from the total concentrations of BOPTA. D. The initial hepatocellular uptake index [IHUI, nmol/min/g] was measured between time 46 and time 48 min. During this 2-min interval, few BOPTA were excreted into bile and the slope of relation between concentrations and time accurately reflects the hepatic uptake of the contrast agent. IHUI in livers perfused with 200 µM BOPTA and no RIF [R_0], 1 µM RIF [R_1], 10 µM RIF [R_{10}], or 100 µM RIF [R_{100}].

Fig. 4. BOPTA transport through hepatocytes. Effects of perfusion solutions on BOPTA bile excretion rates [nmol/min, A], BOPTA concentrations in hepatocytes [nmol/g] (B), and BOPTA efflux rates from hepatocytes back to sinusoids [nmol/min, C] are illustrated. Livers isolated from normal rats and perfused with a Krebs-Henseleit Bicarbonate (KHB) solution from time 10 to time 45 min, 1600 µM BOPTA ± 1 µM rifampicin (RIF) from time 45 to time 75 min, and KHB solution from time 75 to time 105 min: 1600 µM BOPTA alone (B_{1600}, white squares) and 1600 µM BOPTA + 1 µM RIF ($B_{1600}R_1$, black squares). Vertical lines limit the period of drug perfusion.

Fig. 5. Drug-drug interactions through efflux transport proteins. BOPTA bile excretion rates during the drug perfusion period [nmol/min, A], BOPTA bile excretion rates during the KHB perfusion period [nmol/min, B], and BOPTA perfusate efflux rates during the KHB perfusion period [nmol/min, C] are plotted according to the concentrations in hepatocytes (nmol/g). Cellular concentrations were higher during the drug perfusion period (A) that during the KHB perfusion period (B and C). Data from all experimental groups are plotted according to the absence or presence of rifampicin (RIF) in perfused solutions: absence of RIF (blue squares) and presence of RIF (grey squares).

TABLES

Table 1. Rifampicin (RIF) measurements during the rinse period

Experimental groups	Time [min]	Hepatic concentrations [nmol/g]	Bile efflux rates [nmol/min]	Perfusate efflux rates [nmol/min]
100 µM RIF in normal livers	90	380 ± 110	3.3 ± 1.3	216 ± 39
	105	197 ± 64	2.3 ± 0.8	71 ± 31
100 µM RIF in liver lacking Mrp2	90	538 ± 215[1]	0[1]	269 ± 32
	105	270 ± 100[1]	0[1]	85 ± 7
100 µM RIF and 200 µM BOPTA	90	348 ± 194	3.1 ± 0.7	244 ± 61
	105	151 ± 44	2.3 ± 0.7	53 ± 34
10 µM RIF and 200 µM BOPTA	90	103 ± 40	0.9 ± 0.2	58 ± 9
	105	71 ± 19	0.5 ± 0.1	26 ± 9
1 µM RIF and 200 µM BOPTA	90	46 ± 24	0.2 ± 0.1	15 ± 11
	105	22 ± 23	0.1 ± 0.1	7 ± 6

Two time-points are available: times 90 and 105 min. [1] $p = 0.05$ vs. 100 µM RIF in normal livers (with Mrp2)

Fig. 1

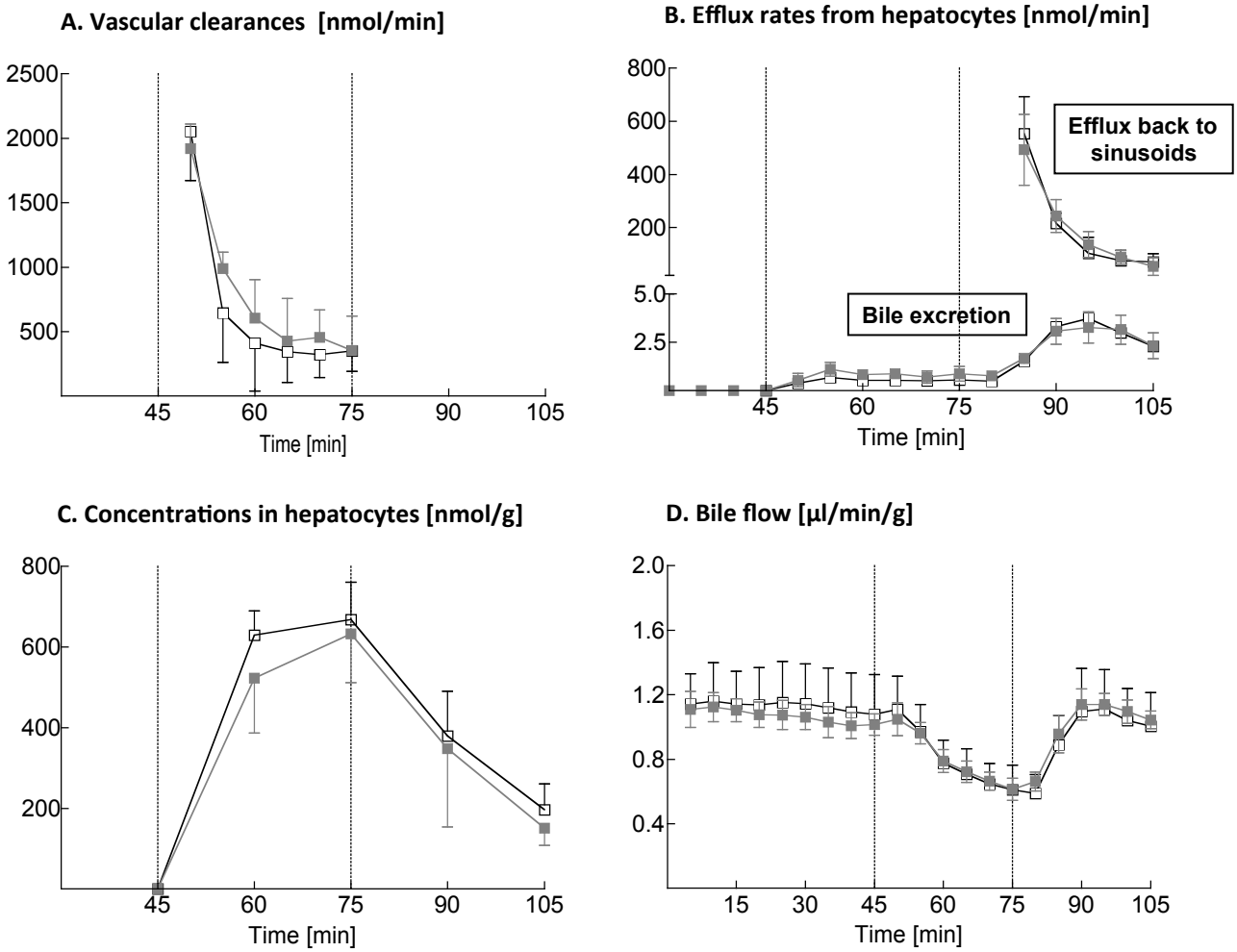

Fig. 2

DMD Fast Forward. Published on May 24, 2013 as DOI: 10.1124/dmd.113.051870

A. Vascular clearances [nmol/min]

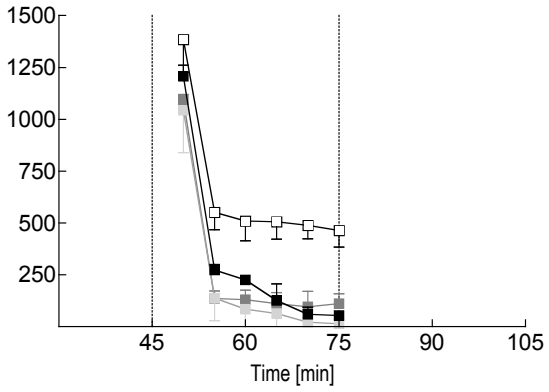

B. BOPTA bile excretion rates [nmol/min]

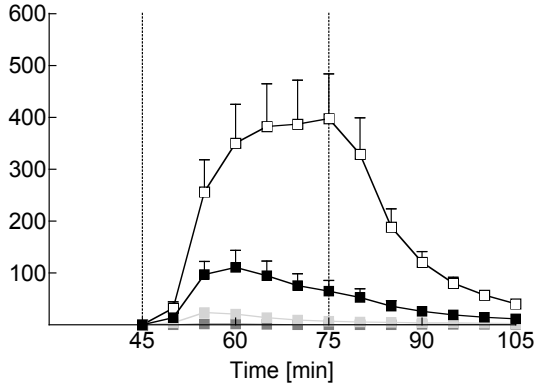

C. BOPTA efflux back to sinusoids [nmol/min]

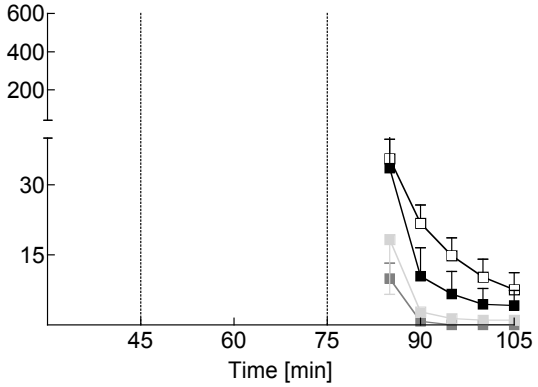

D. BOPTA Concentrations in hepatocytes [nmol/g]

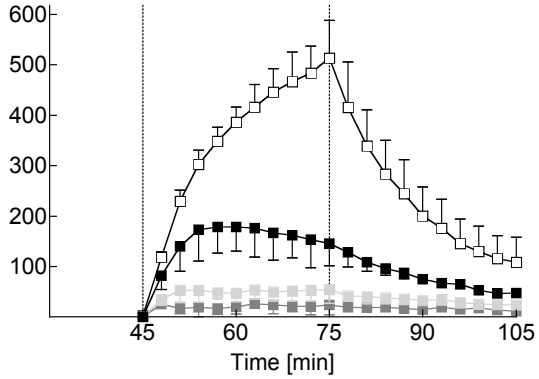

Fig. 3

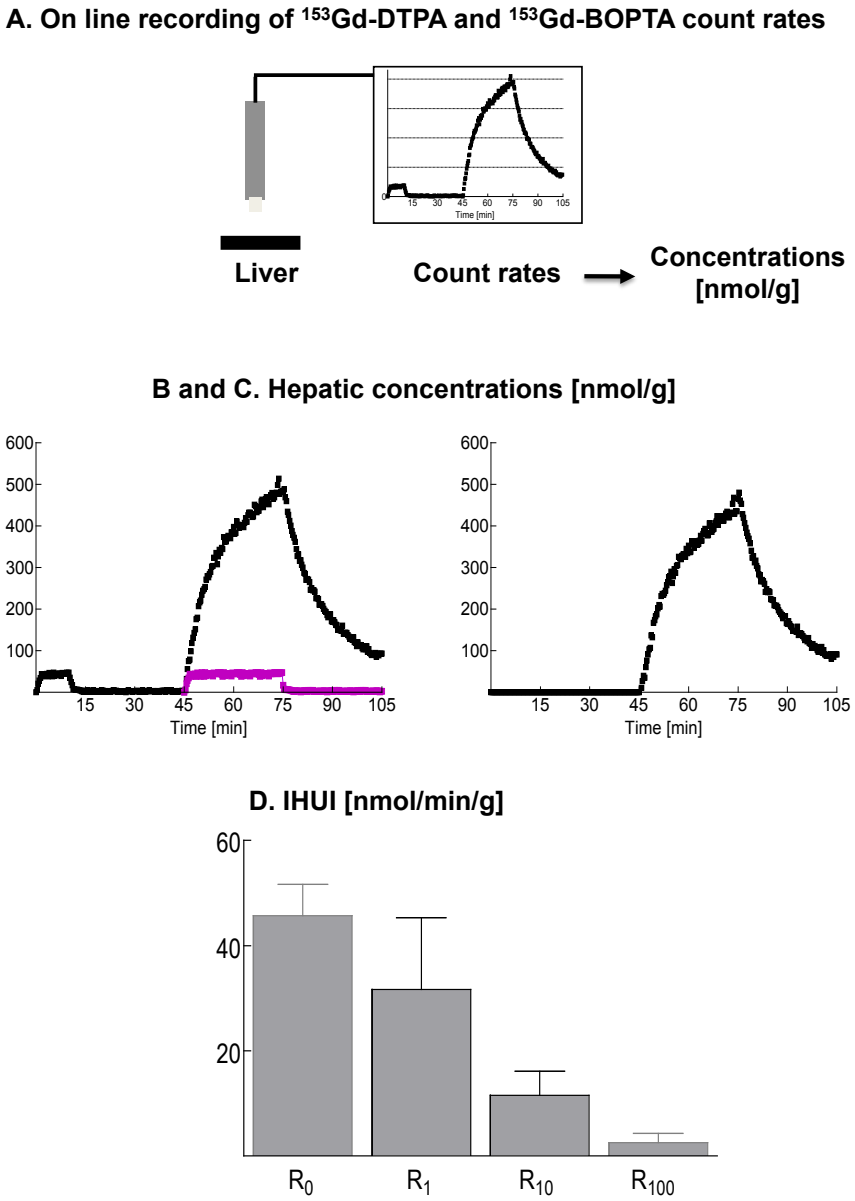

Fig. 4

DMD Fast Forward. Published on May 24, 2013 as DOI: 10.1124/dmd.113.051870
This article has not been copyedited and formatted. The final version may differ from this version.

A. BOPTA bile excretion rates [nmol/min]

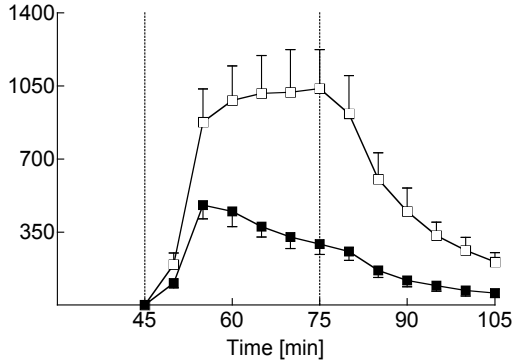

B. BOPTA concentrations in hepatocytes [nmol/g]

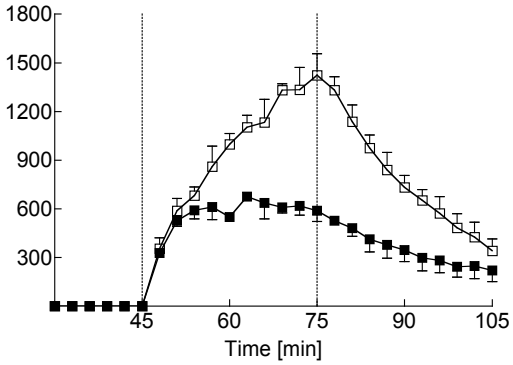

C. BOPTA efflux back to sinusoids [nmol/min]

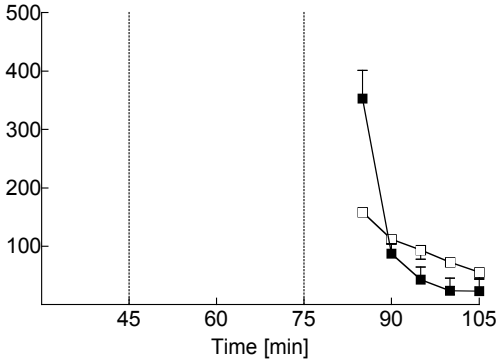

Fig. 5

DMD Fast Forward. Published on May 24, 2013 as DOI: 10.1124/dmd.113.051870
This article has not been copyedited and formatted. The final version may differ from this version.

A. Bile excretion rates during drug perfusion

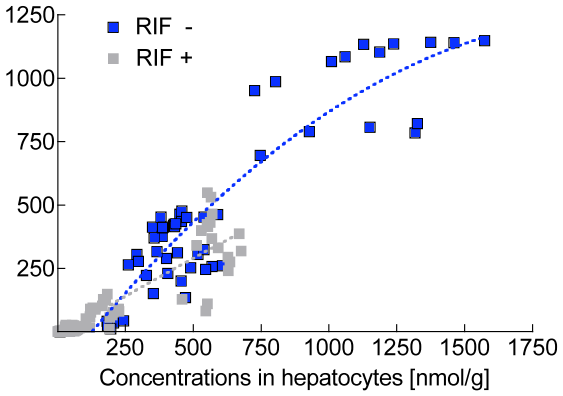

B. Bile excretion rates during KHB period

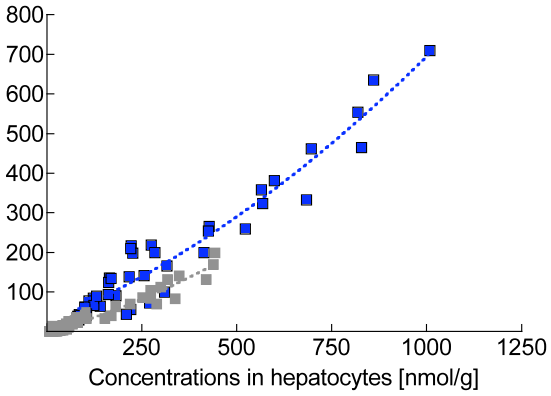

C. Perfusate efflux rates during KHB period